Crossing the Barrier: When the Diaphragm Is Not A Limit

Leonardo Lidid[1]
Juan Valenzuela[1]
Carlos Villarroel[1]
Julia Alegria[2]

OBJECTIVE. The purpose of this article is to depict the anatomic pathways along which transphrenic spread of diseases and entities can disseminate.

CONCLUSION. The abdomen and thorax form a continuum on which the diaphragm is an important but incomplete barrier to disease migration.

The concept of the diaphragm as a barrier is a widespread and tacitly accepted, though misunderstood, concept shared by many physicians. The presence of multiple transphrenic pathways and the various diseases traveling them are relatively unknown, which translates into mistakes and severe diagnostic delays. The purpose of this essay is to depict these anatomic constitutional pathways and the diseases that can take these routes in adults. The pathways encompass both congenital communications and those occurring in areas of structural weakness of embryologic origin that have a degree of acquired component [1, 2]. The other group of migrations, that is, purely acquired spread (e.g., iatrogenic and traumatic), does not necessarily travel along these pathways and is not discussed.

Embryology of the Diaphragm and Subserosal Space

The coelomic cavity is formed at the end of the third week of embryonic life and is lined by a serous membrane. Deep to it lies the subserosal space, which can be conceptualized as one continuous space from thorax (subpleural space) to abdomen (subperitoneal space) (Fig. 1). The thoracoabdominal continuum is that portion of the subserous space that crosses the diaphragmatic hiatuses and connects these two areas, allowing both the passage of vital structures and bidirectional disease migration [3, 4].

Anatomic Pathways

Traditionally, the esophageal, aortic, and Morgagni hiatuses have been described as subserous connections. Nevertheless, other potential pathways of transphrenic spread are as follows: lumbocostal triangle, caval foramen, phrenic lymphatic vessels, and tiny diaphragmatic defects (porous diaphragm syndrome) [1–3, 5–8] (Fig. 2A). Although the idea is controversial, many authors consider the aortic and esophageal hiatuses the most common diaphragmatic communication pathways [2–4, 9].

Aortic Hiatus

Many anatomic structures run through the aortic hiatus (Fig. 2B). Thus pathologic processes affecting these structures can freely spread by this route, as in the case of lymphatic neoplastic dissemination [1, 3, 4] (Fig. 3). In addition, through retrocrural fat, numerous processes, including air (pneumomediastinum) and fluid collection (urine and blood, among others) can spread bidirectionally [3, 4, 9] (Fig. 4).

Esophageal Hiatus

The esophageal hiatus, partly because of its connection with the hepatic bare area, represents an important route of transphrenic dissemination, as seen in some cases of thoracic fistula of pancreatic pseudocysts [2, 3, 9, 10] (Fig. 5).

In the bare area, the esophageal hiatus, gastrohepatic ligament, and retroperitoneum appear interconnected [5, 11] (Fig. 6), and the continuity may extend even to the pelvic extraperitoneal space [4, 9, 11, 12] (Fig. 7). Furthermore, the presence of another transphrenic connection, the caval foramen (Fig. 6), turns the bare area into a crossroads of transdiaphragmatic disease dissemination (Fig. 8).

Hiatal hernia—the most common condition affecting the esophageal hiatus—can

Keywords: congenital diaphragmatic hernia, diaphragm, embryology, peritoneum, retroperitoneal space

DOI:10.2214/AJR.11.8264

Received November 13, 2011; accepted after revision July 18, 2012.

[1]Department of Radiology, Universidad de Chile, Campus Occidente, Facultad de medicine, Hospital San Juan de Dios, Avenida Portales 3239, Santiago, Chile 8350533. Address correspondence to L. Lidid (leolidid@gmail.com).

[2]Department of Radiology, Universidad del Desarrollo, Facultad de medicine, Clinica Alemana de Santiago, Santiago, Chile.

WEB
This is a Web exclusive article.

AJR 2013; 200:W62–W70

0361–803X/13/2001–W62

contain a variety of structures from stomach to colon [5, 13] (Fig. 9). Any component can be affected by different diseases, which can involve the hernial sac (Fig. 10) and extend beyond it. Gastropleural fistulas secondary to this alteration have been reported [10].

Vena Caval Foramen

The vena caval foramen is not considered part of the continuum because its adherence to the vein wall does not allow subserous tissue [3]. Nevertheless, this foramen has occasionally been described as a potential pathway for bidirectional disease migration, both in retroperitoneal abscesses [11] and in cases of descending mediastinitis [14]. In addition, the caval lumen by itself can act as a transphrenic pathway, usually described in (macroscopic) transvenous spread of some neoplastic diseases [4] (Fig. 11).

Morgagni Hiatus

A Morgagni hiatus is a small bilateral ventral aperture (Fig. 2A) across which superior epigastric and lymph vessels from the diaphragmatic aspect of the liver travel. Many processes, including subperitoneal air, can travel this way [3, 4, 10] (Fig. 12). The rarely observed Morgagni hernia can also develop at this hiatus, frequently on the right side, when there is a genesis of its attachments, especially of the xiphoid extension [6, 13] (Fig. 9).

Lumbocostal Triangle and Septum Transversum Lacunar Aplasia

A defect in formation of the posterolateral margin of the diaphragmatic surface usually results in Bochdalek hernia [2, 7, 13] (Fig. 2A). Usually left-sided, this hernia may contain fat only and can be asymptomatic in adults; nevertheless, it can contain part of the kidney, stomach, and even bowel [13] (Fig. 13). Finally, the extremely rare peritoneal pericardial hernia (septum transversum lacunar aplasia) can develop at the diaphragmatic central tendon [6] (Fig. 2A). Noteworthy is that the last two hernias and, to a lesser extent, Morgagni hernia can lack a hernial sac [6, 13].

Porous Diaphragm Syndromes

Porous diaphragm syndromes are a group of different diseases with a common cause, that is, a tiny focal defect in the diaphragm that allows transphrenic migration of substances (fluids, gases, neoplasms, tissues, exudates, and even infected ascitic fluid) from the peritoneal cavity into the pleural spaces. The tendinous part of the diaphragm is the most common site of defects. The defects can correspond to pleuroperitoneal bleb (a small hole with a pleuroperitoneal cover and blister morphologic features), fenestrations (rupture of a previous bleb), or multiple gaps (cribriform diaphragm). These anomalies can be congenital or acquired and for various reasons (peritoneal circulation, piston effect of the liver), right-sided thoracic involvement is more common [1, 5, 15] (Fig. 2A). Meigs syndrome—fibroma or fibromalike benign ovarian tumor, ascites, pleural effusion (usually right-sided), and hydrothorax managed by removal of the ovarian tumor—appears to be the quintessential example of a porous diaphragm syndrome [5]. Catamenial pneumothorax is another example. It presents as spontaneous pneumothorax, usually right-sided, occurring with the onset of menses [1, 5]. Hepatic hydrothorax, or the presence of substantial pleural effusion in patients with liver disease (without underlying cardiovascular conditions), traditionally has been included in this category along with the occurrence of pleural effusion in peritoneal dialysis patients, among others [5, 10].

Detection of these defects is relevant when treatment of the primary pathologic process fails and surgical management seems advisable. The diagnosis can be made by intraperitoneal administration of ^{99m}Tc–sulfur colloid and with ultrasound, CT (Fig. 14), and MRI, although other medical procedures (thoracoscopy, dye use) are also being used [1, 5, 15].

Diaphragmatic Lymphatics

The diaphragm has a lymphatic drainage system (Fig. 15), which explains the widely known neoplastic dissemination that can occur between the thorax and the abdomen [4, 7, 8]. However, evidence from animal and human models suggests that both proteins and particulate matter cross the diaphragm via transdiaphragmatic and pleural lymphatic vessels [1]. This route, although debatable [9], has been proposed as an alternative and complementary explanation for porous diaphragmatic syndrome, along with the diaphragmatic defects already described [1, 4, 9, 10, 15].

Conclusion

Pathologic processes have many routes through the diaphragm. Consequently, the chest and abdominal cavities can be seen as a continuum on which the diaphragm is an important—but by no means complete—barrier to disease spread.

Acknowledgments

We thank Patricia Guzmán, Marco Barbieri, Ignacio Maldonado, Mario Mora, Fabiola Vargas, and all residents of the San Juan Radiology Department. We also thank Antonio Pinto for his fine artwork.

References

1. Panicek DM, Benson CB, Gottlieb RH, Heitzman ER. The diaphragm: anatomic, pathologic, and radiologic considerations. *RadioGraphics* 1988; 8: 385–425
2. Müller NL, Webb WR, Müller NL, Vlahos I, Krinsky GA. *Computed tomography and magnetic resonance of the thorax*, 4th ed. Philadelphia, PA: Lippincott Williams and Wilkins, 2007:863–874
3. Oliphant M, Berne AS, Meyers MA. The subserous thoracoabdominal continuum: embryologic basis and diagnostic imaging of disease spread. *Abdom Imaging* 1999; 24:211–219
4. Meyers MA, Charnsangavej C, Oliphant M. *Meyers' dynamic radiology of the abdomen: normal and pathologic anatomy,* 6th ed. New York, NY: Springer, 2011
5. Sugarbaker DJ, Bueno R, Krasna M, Mentzer SJ, Zellos L. *Adult chest surgery.* New York, NY: McGraw Hill, 2009
6. Arráez-Aybar LA, González-Gómez CC, Torres-García AJ. Morgagni-Larrey paraesternal diaphragmatic hernia in the adult. *Rev Esp Enferm Dig* 2009; 101:357–366
7. Rouvière H, Delmas A, Delmas V. *Anatomía humana: descriptiva, topográfica y funcional*, 11th ed, vol 2. Barcelona, Spain: Masson, 2006
8. Moore K, Dalley A. *Clinically oriented anatomy,* 6th ed. Philadelphia, PA. Lippincott Williams and Wilkins, 2010
9. Akpek S, Gore R. Another route for escape. *AJR* 2001; 176:1601–1602
10. Sahn SA. Pleural effusions of extravascular origin. *Clin Chest Med* 2006; 27:285–308
11. Domjan JM, Tung KT, Johnson C. Bare area abscess: imaging findings and potential communication with the mediastinum. *Br J Radiol* 1997; 70:754–757
12. Lim JH, Kim B, Auh YH. Anatomical communications of the perirenal space. *Br J Radiol* 1998; 71:450–456
13. Müller NL, Silva IS. *High-yield imaging: chest.* Philadelphia, PA: Saunders Elsevier, 2010
14. Cirino LM, Elias FM, Almeida JL. Descending mediastinitis: a review. *Sao Paulo Med J* 2006; 124:285–290
15. Kiafar C, Gilani N. Hepatic hydrothorax: current concepts of pathophysiology and treatment options. *Ann Hepatol* 2008; 7:313–320

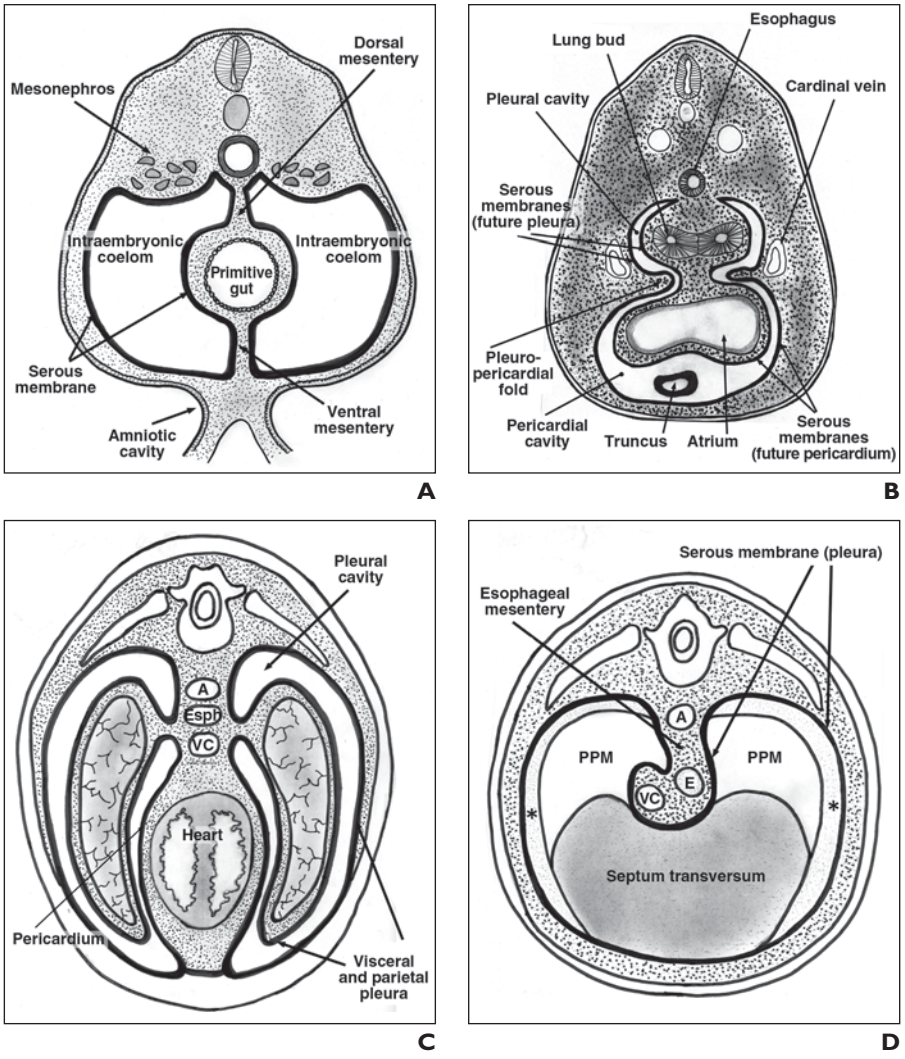

Fig. 1—Embryologic features of diaphragm and subserous space. Schemas show axial cut of embryo at different stages of gestation. Intraembryonic coelom (large cavity extending from thorax to pelvis) is lined by serous membrane (*thick black line*), and under it lies subserous space (*stippled area*).
A, 4-week embryo. Developing organs (e.g., gut) are subjacent to serous lining and project into coelomic cavity. Septum transversum (future diaphragm) will grow from ventral wall and partially divide coelom into eventual thoracic and abdominal cavities.
B, 4- to 5-week embryo. At thoracic level, lung buds grow from primitive gut covered by serous membrane. Heart is also being formed.
C, 5-week embryo. Lungs grow into pleural cavity (legacy of coelomic cavity). A = aorta, Esph = esophagus, VC = vena cava.
D, 7-week embryo. Division of pleural and peritoneal cavities complete with pleuroperitoneal membranes (PPM) that grow from every side of posterior wall, closing dorsal openings and fusing with septum transversum and esophageal mesentery. Esophageal mesentery forms stippled area that contains esophagus (E) and vena cava (VC). Later, growth of muscular body wall (*asterisks*) completes periphery of diaphragm, except at ventral small (Morgagni) hiatuses. A = aorta.

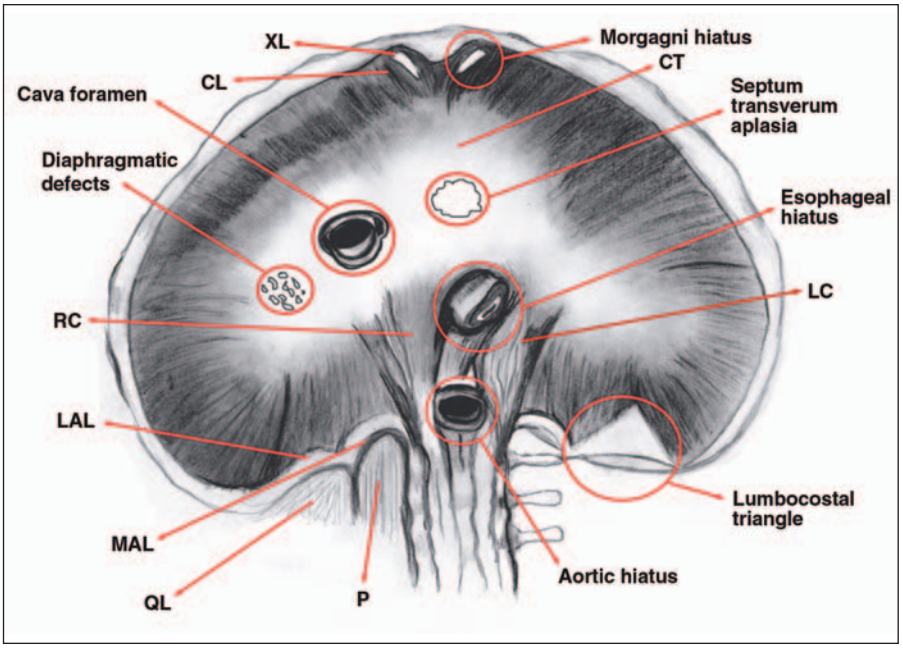

A

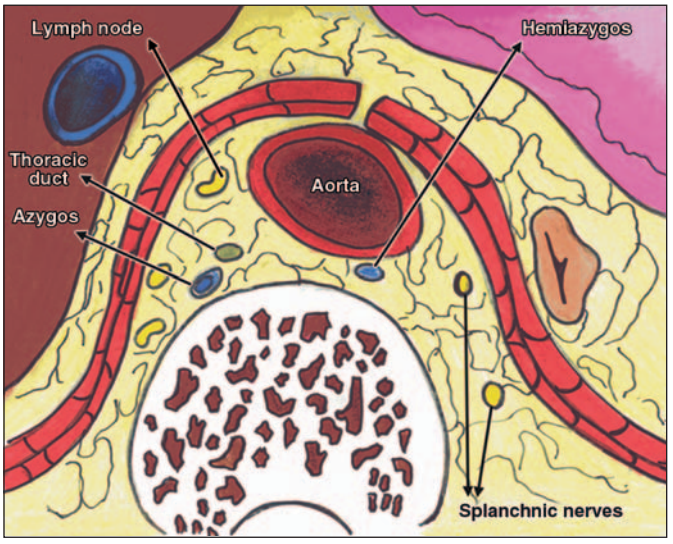

B

Fig. 2—Schema of transphrenic pathway.
A, Caudal view of diaphragm shows constitutional transphrenic pathways encircled: aortic, esophageal, and Morgagni hiatuses; foramen of vena cava; lumbocostal triangle (Bochdalek hernia); septum transversum lacunar aplasia (peritoneal pericardial hernia); diaphragmatic defects (porous diaphragm syndrome); and transphrenic lymphatic vessels (not shown). Esophageal and aortic hiatuses are between right (RC) and left (LC) crura. Morgagni hiatus is between xiphoid (XL) and costal (CL) attachments. Lumbocostal triangle is area of diaphragmatic thinning related to ligamentum arcuatum laterale (LAL), frequently presenting incomplete development. Other communications can occur in different sites of central tendon (CT). MAL = medial arcuate ligament, P = psoas muscle, QL = quadratus lumborum muscle on right, excised on left.
B, Axial view shows aortic hiatus and its content.

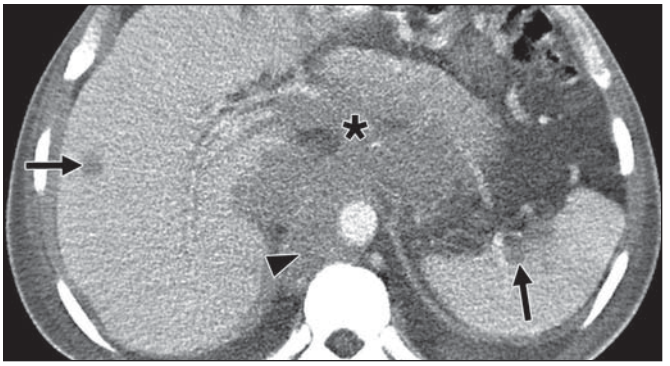

Fig. 3—34-year-old man with aggressive testicular seminomatous tumor and multiple lymphadenopathies. Axial contrast-enhanced CT scan shows extensive retrocrural (*arrowhead*) and celiac trunk (*asterisk*) adenopathies, among others, and hepatic (*right arrow*) and splenic (*left arrow*) metastasis.

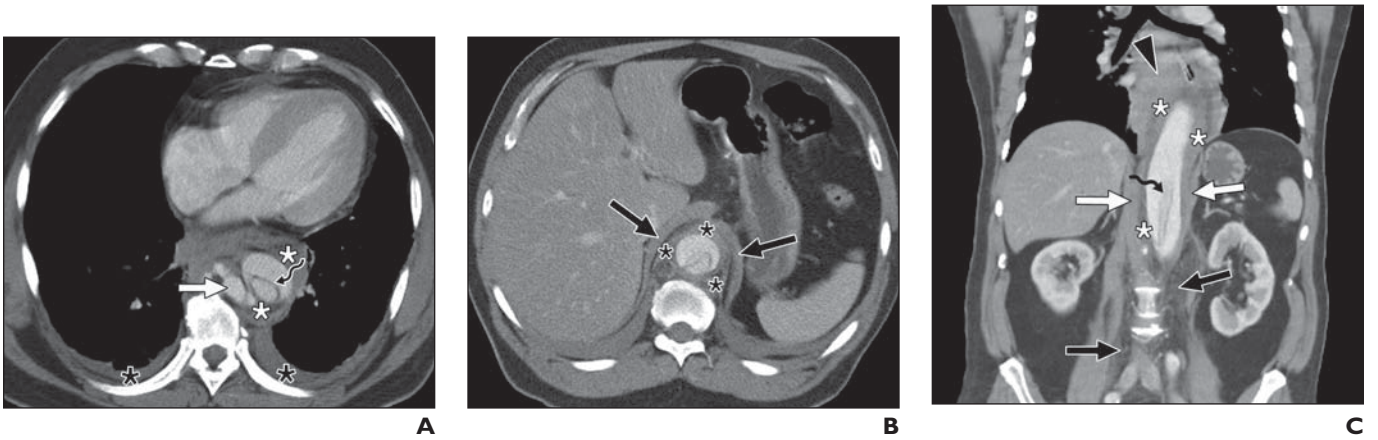

Fig. 4—54-year-old man with ruptured descending thoracic aortic dissection and retrocrural, and retroperitoneal blood extension.
A, Axial contrast-enhanced CT image of chest shows aortic dissection (*wavy arrow*) with active contrast extravasation into lower thoracic aortic segment (*straight arrow*). Blood is present in mediastinal periaortic fat (*white asterisks*) and both pleural spaces (*black asterisks*).
B, Axial contrast-enhanced CT image of thoracoabdominal segment shows extension of blood (*asterisks*) into retrocrural space (*arrows*).
C, Coronal maximum-intensity-projection contrast-enhanced CT image shows dissection flap (*wavy arrow*) and mediastinal (*arrowhead*) and periaortic (*asterisks*) blood accumulation between crura (*white arrows*) and reaching retroperitoneum (*black arrows*).

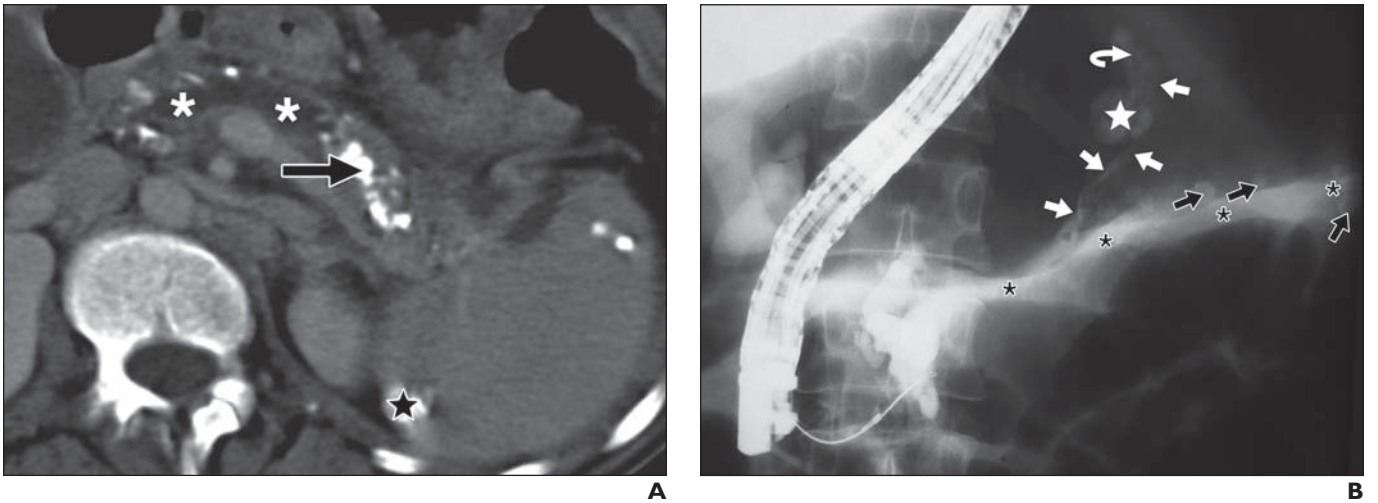

Fig. 5—40-year-old woman with chronic pancreatitis and thoracic pseudocyst fistulization.
A, Axial oblique maximum-intensity-projection contrast-enhanced 4-MDCT image shows ductal dilatation (*asterisks*) and pancreatic calcifications (*arrow*). Large splenic calcified granuloma (*star*) is evident.
B, Frontal ERCP image shows dilated duct of Wirsung (*asterisks*) and fistulous track (*white straight arrows*) that communicates to more cephalic intraabdominal collection (*curved arrow*). Splenic granuloma (*star*) and pancreatic calcification (*black arrows*) are evident.

(Fig. 5 continues on next page)

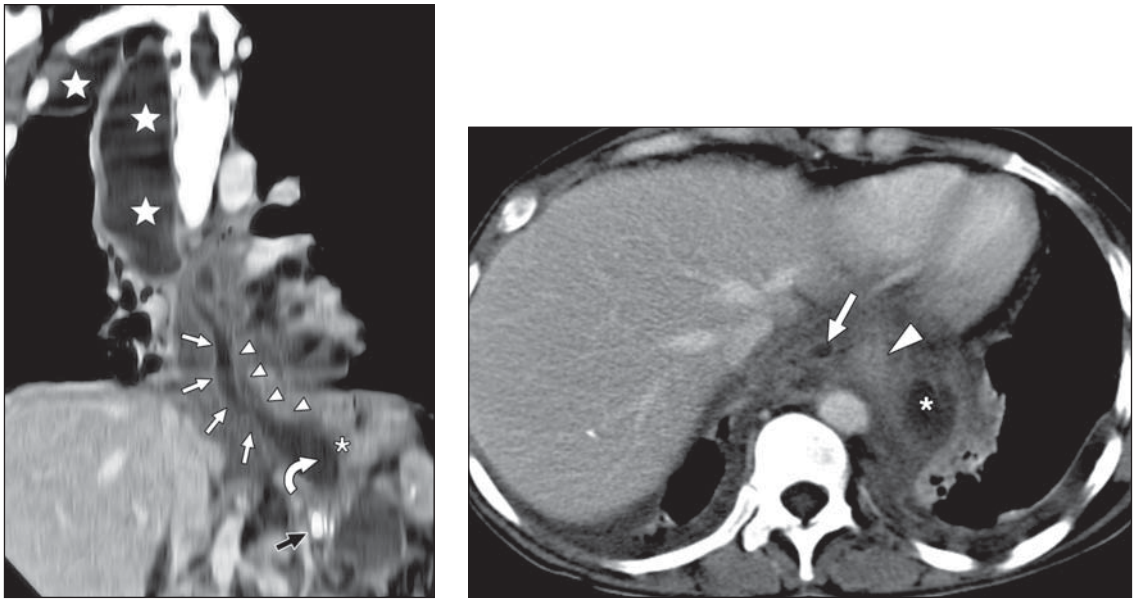

Fig. 5 (continued)—40-year-old woman with chronic pancreatitis and thoracic pseudocyst fistulization.
C, Curved coronal average-intensity-projection contrast-enhanced 4-MDCT image at level of esophageal hiatus shows previous collection corresponding to pseudocyst (*curved arrow*) at lesser curvature of stomach (*asterisk*) in continuity with fistulous track (*white straight arrows*) that parallels esophagus (*arrowheads*) and determines several collections in mediastinal and pleural spaces (*stars*). Pancreatic calcifications (*black arrow*) are evident.
D, Axial contrast-enhanced 4-MDCT image of lower mediastinum depicts right paraesophageal pathway (*arrow*) and mediastinal collection (*asterisk*). Arrowhead indicates esophagus. Pancreatic thoracic fistulization is uncommon and when it occurs is generally related to chronic alcoholic pancreatitis. ERCP, MRCP, or CT may be used for imaging.

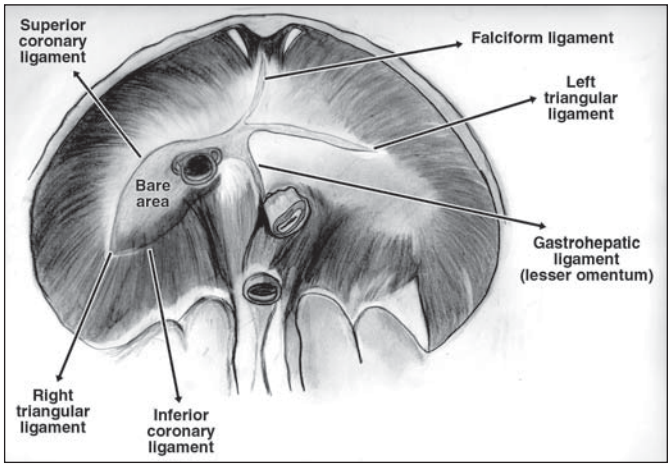

Fig. 6—Limits and communications of bare area of liver. Drawing shows caudal side of diaphragm. Among main communications in this region, retroperitoneum, esophageal hiatus and lesser omentum, and foramen of vena cava have to be considered. Compare with Figure 2A.

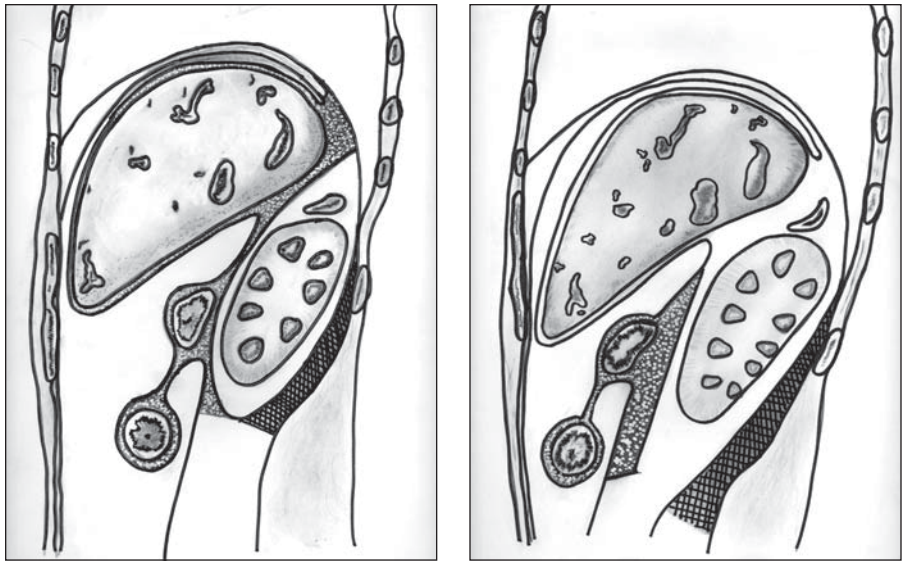

Fig. 7—Continuity of hepatic bare area and retroperitoneum. Discrepancies in anatomic conception among authors have been reported.
A, Meyers concept. Schematic sagittal section through liver and right kidney shows renal fasciae are closed above and below kidney and adrenal glands. Right anterior pararenal space (*stippled*) is in continuity with bare area of liver. Posterior pararenal space (*cross-hatched*) is limited by superior fusion of renal fasciae.
B, Other concepts. Schematic sagittal section through liver and right kidney shows superior aspect of perirenal space (*white*) is wide open in continuity with bare area on right and limited by extrapleural diaphragmatic dome on left. Inferior apex of renal cone is open with caudal extension out of perirenal space. Pararenal spaces do not extend to bare area or diaphragmatic dome.

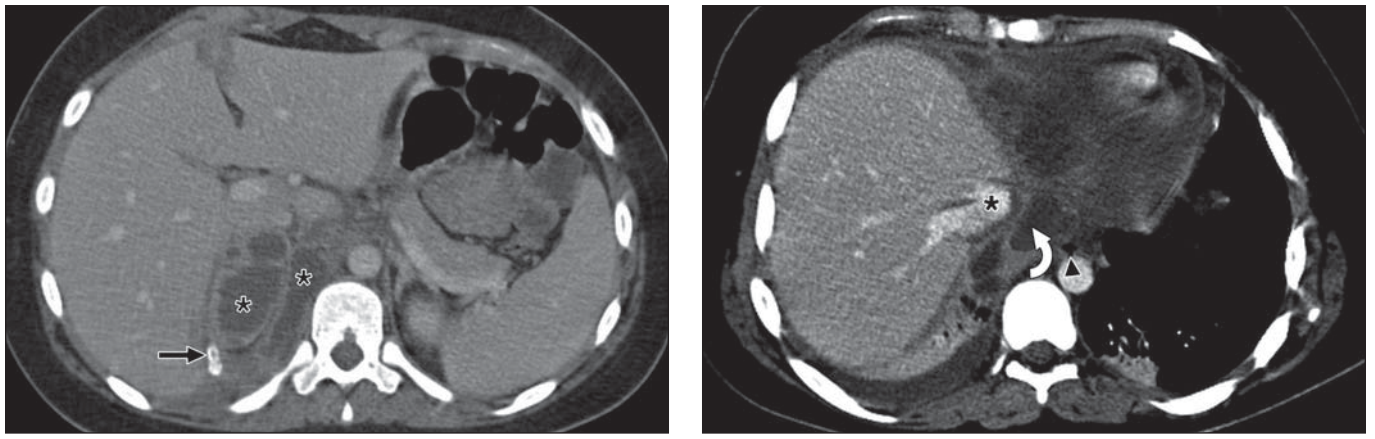

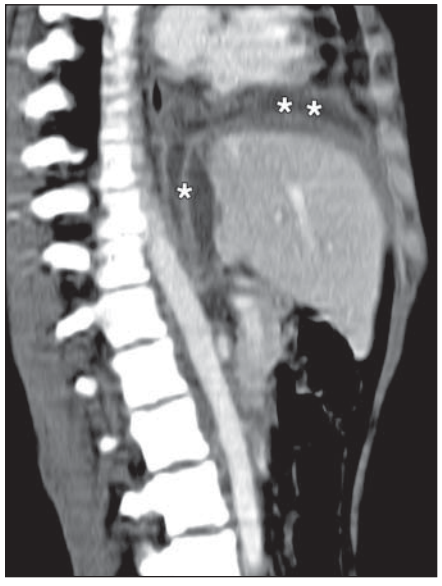

Fig. 8—15-year-old girl who underwent classic appendectomy and was readmitted 1 month later with proximal psoas abscess progression (not shown) and retrohepatic collection.
A, Axial average-intensity-projection contrast-enhanced CT image shows two appendoliths (*arrow*) and one abscess (*asterisks*) in bare area of liver.
B. Axial average-intensity-projection contrast-enhanced CT image cephalic to **A** shows no clear evidence that collection goes through vena caval foramen (*asterisk*) or esophageal hiatus (*arrowhead*) but does show cephalic extension of abscess at thoracoabdominal diaphragmatic transition (*curved arrow*).
C, Right oblique parasagittal average-intensity-projection contrast-enhanced CT image shows continuum of retrohepatic (*single asterisk*) and supradiaphragmatic (*double asterisks*) collections.

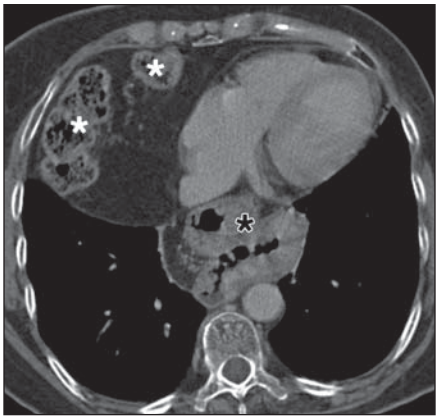

A

B

Fig. 9—67-year-old woman with hiatal and Morgagni hernias.
A, Axial contrast-enhanced CT image of chest shows Morgagni hernia on right containing transverse colon (*white asterisks*) and epiploon and a sliding hiatal hernia with gastric fundus in mediastinum (*black asterisk*).
B, Oblique sagittal average-intensity-projection contrast-enhanced CT image depicts hiatal hernia foramen (*arrows*) and enlarged right Morgagni hiatus (*arrowheads*) through which epiploon and colonic loop run.

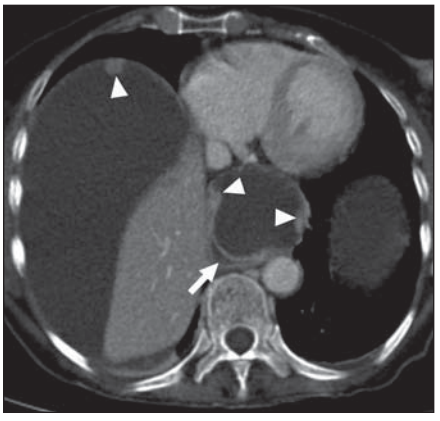

Fig. 10—77-year-old woman with ovarian peritoneal mucinous carcinomatosis, hiatal hernia, and hernial sac implants. Axial contrast-enhanced CT image depicts nodules (*arrowheads*) of peritoneal carcinomatosis in abdominal side of diaphragm and at hiatal hernial sac. Esophagus in hernia is displaced backward by mucinous content (*arrow*).

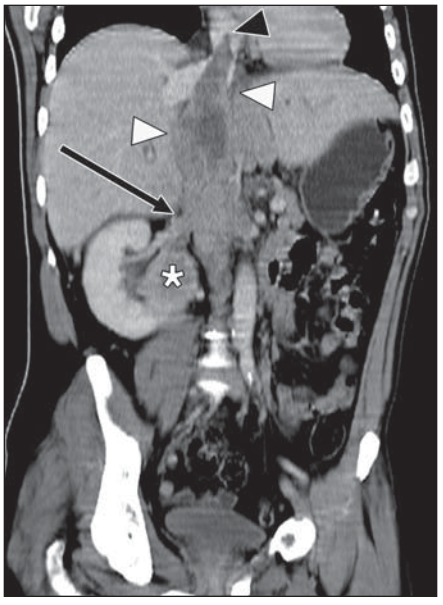

Fig. 11—47-year-old man with hematuria caused by hypernephroma with supradiaphragmatic vena caval invasion. Oblique coronal average-intensity-projection contrast-enhanced CT image depicts renal cell carcinoma (*asterisk*) with extension of mixed soft tumoral thrombus into right renal vein (*arrow*), inferior vena cava, and right atrium (*arrowheads*). Other tumors with common transvenous caval dissemination are hepatocellular and adrenal carcinomas and, infrequently, caval leiomyosarcoma.

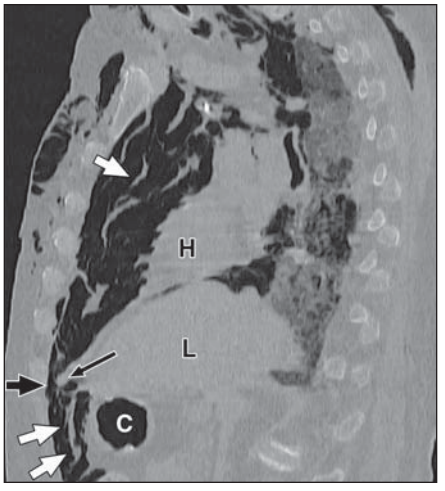

Fig. 12—61-year-old woman with abdominal extension of pneumomediastinum. Parasagittal multiplanar reconstruction 4-MDCT image at level of Morgagni hiatus shows pneumomediastinum and extrapleural (subpleural) air (*single white arrow*) with extension through this hiatus (*thick black arrow*) toward abdominal subperitoneal space (*double white arrows*). Compare with Figures 9B and 15. This dissemination can follow other routes, such as esophageal and aortic hiatuses. Presence of upward flow, as in cases of transphrenic migration of air in laparoscopic surgical procedures and intestinal perforation, has been described. Thin black arrow indicates diaphragmatic tip of Morgagni hiatus.
H = heart, L = liver, C= colon.

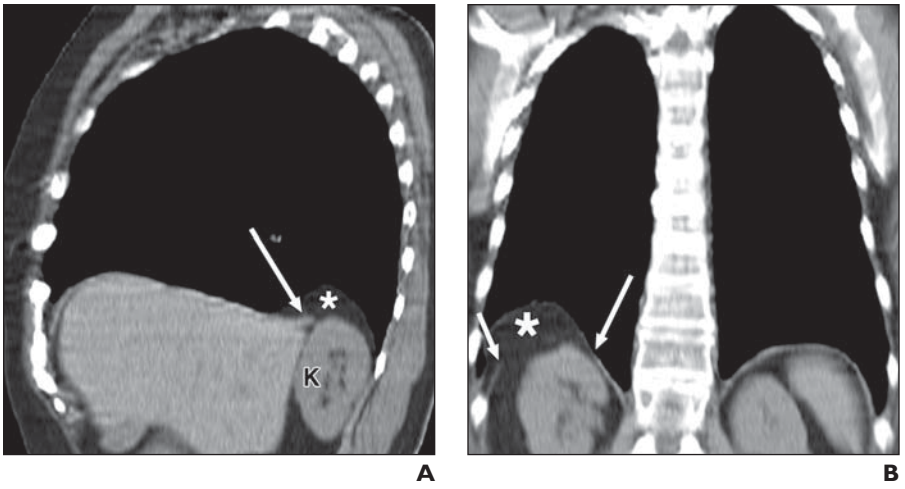

Fig. 13—80-year-old woman with ascension of kidney through right Bochdalek hernia.
A, Right sagittal average-intensity-projection CT image shows tip of diaphragmatic defect (*arrow*) with absence of posterior insertion, herniation of retroperitoneal fat (*asterisk*), and superior pole of right kidney (K).
B, Coronal average-intensity-projection CT image depicts diaphragmatic defect in posterolateral aspect of diaphragm (*arrows*) with herniation of same retroperitoneal content (*asterisk*). Compare with Figure 2A.

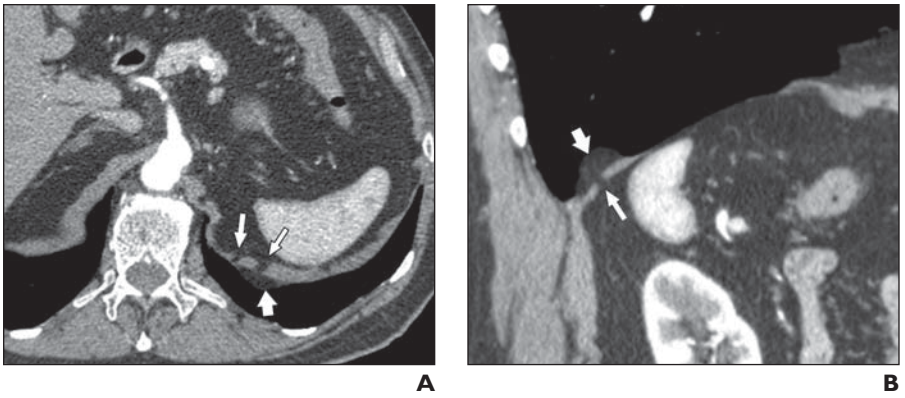

Fig. 14—86-year-old man with left diaphragmatic defects.
A, Axial contrast-enhanced CT image of chest shows two small defects (*thin arrows*) in posteromedial aspect of left diaphragmatic dome. Tiny amount of abdominal fat (*thick arrow*) is herniating through them.
B, Sagittal multiplanar reconstruction CT image shows one of defects (*arrows*) described in **A.** Normal dorsal diaphragmatic insertion is present behind it.

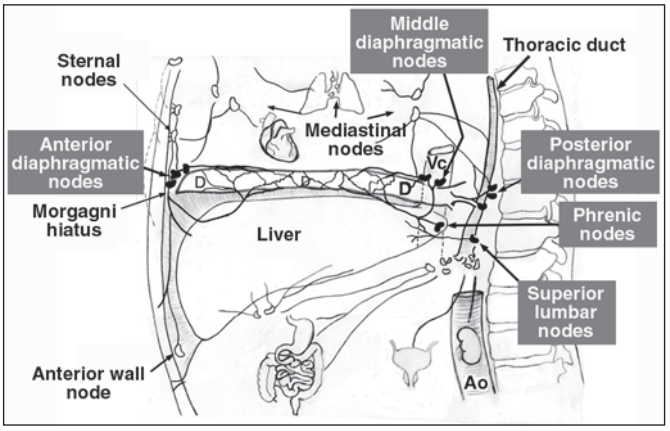

Fig. 15—Diaphragmatic lymphatic system. Sagittal diagram shows lymphatic vessels (*black lines*) are formed in two plexuses, on each side of diaphragm (D) with free (intrinsic microscopic) communications between them. In addition, each side of diaphragm is drained both by common nodal groups (anterior and middle diaphragmatic lymph nodes) and by nodes specific to each side: thoracic, posterior (retrocrural) diaphragmatic lymph nodes, and abdominal, phrenic, and lumbar lymph nodes. Thoracic duct allows communication between nodes of abdominal and thoracic regions. Lymphatics have been proposed as transphrenic dissemination pathway for multiple phenomena, including neoplasms, septic processes, urinothorax, and porous diaphragm syndromes. Vc = vena cava, Ao = aorta.